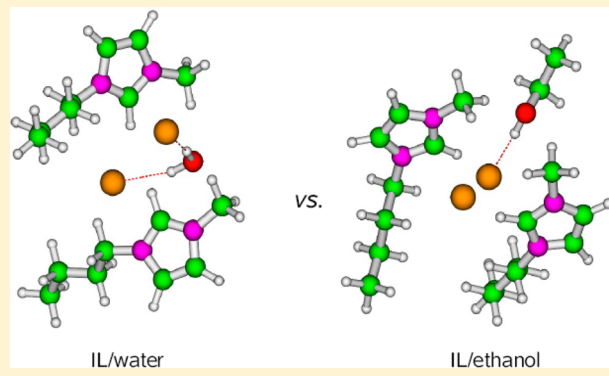


# Understanding the Role of the Cosolvent in the Zeolite Template Function of Imidazolium-Based Ionic Liquid

Regla Ayala,\* Svetlana Ivanova, José María Martínez Blanes, Francisca Romero-Sarria, and José Antonio Odriozola

Departamento de Química Inorgánica e Instituto de Ciencia de Materiales de Sevilla, Universidad de Sevilla-CSIC, Avenida Américo Vespucio 441092 Sevilla, Spain

**ABSTRACT:** In this work, a study for understanding the role played by  $[\text{ClBmim}]$ ,  $[\text{BF}_4\text{Bmim}]$ ,  $[\text{PF}_6\text{Bmim}]$ , and  $[\text{CH}_3\text{SO}_3\text{Bmim}]$  ionic liquids (ILs) in the synthesis of zeolites is presented. The use of  $[\text{ClBmim}]$  and  $[\text{CH}_3\text{SO}_3\text{Bmim}]$  ILs, as reported earlier [*Chem. Eur. J.* 2013, 19, 2122] led to the formation of MFI or BEA type zeolites. Contrary,  $[\text{BF}_4\text{Bmim}]$  and  $[\text{PF}_6\text{Bmim}]$  ILs did not succeed in organizing the Si-Al network into a zeolite structure. To try to explain these results, a series of quantum mechanical calculations considering monomers ( $[\text{XBmim}]$ ) and dimers ( $[\text{XBmim}]_2$ ) by themselves and plus cosolvent (water or ethanol) were carried out, where  $\text{X} \equiv \text{Cl}^-$ ,  $\text{BF}_4^-$ ,  $\text{PF}_6^-$ , or  $\text{CH}_3\text{SO}_3^-$ . Our attention was focused on the similarities and differences among the two types of cosolvents and the relation between the structure and the multiple factors defining the interactions among the ILs and the cosolvent. Although a specific pattern based on local structures explaining the different behavior of these ILs as a zeolite structuring template was not found, the calculated interaction energies involving the  $\text{Cl}^-$  and  $\text{CH}_3\text{SO}_3^-$  anions were very close and larger than those for  $\text{BF}_4^-$  and  $\text{PF}_6^-$  species. These differences in energy can be used as an argument to describe their different behavior as structure directing agents. Moreover, the topology of the cosolvent is also an ingredient to take into account for a proper understanding of the results.



## INTRODUCTION

The versatile nature of the ionic liquids (ILs) allows their double featuring as solvents and templates in the inorganic materials synthesis. Several examples are available describing their use in the preparation of ordered mesoporous materials<sup>1–5</sup> or zeolites.<sup>5–10</sup> Recently, the use of  $[\text{ClBmim}]$  and  $[\text{CH}_3\text{SO}_3\text{Bmim}]$  (where Bmim means 1-butyl-3-methylimidazolium) ILs for the synthesis of BEA and MFI family zeolites has been published.<sup>11</sup> In this work, it was found that the silicon source determines the formation of zeolites. Depending on the source, different preorganized complexes were obtained that drove the formation of different zeolite families. In the presence of ethanol (released from the TEOS Si-source), the ionic liquid drove to the formation of MFI, and in its absence the BEA type zeolite was obtained. The interactions between the ionic liquid and its immediate chemical environment (water and/or ethanol molecules) were reported to be the crucial factor for the ILs templating function in the zeolite structure formation. Thus, it is interesting to get insight into the nature of water/IL and ethanol/IL mixtures. In this context, the properties of imidazolium-based ILs vary from being completely miscible with water (hydrophilic) to liquids immiscible with water (hydrophobic).<sup>12</sup> As a rule, hydrophobicity increases with the length of the alkyl side chain for the cation and is higher for larger anions, such as  $\text{PF}_6^-$  than for

small ones like  $\text{Cl}^-$ .<sup>13–15</sup> The selection of the anion is usually considered as the primary factor modulating the interaction between ILs and water or other cosolvent.<sup>12</sup> It has been observed that in the case of imidazolium-based ILs,  $\text{PF}_6^-$  salts dissolve less water than  $\text{BF}_4^-$  salts while  $\text{Cl}^-$  and  $\text{CH}_3\text{SO}_3^-$  salts are completely miscible in it.<sup>12,16</sup> These differences in hydrophobicity can have important implications on the ILs role as templates. For this respect, it is worth testing  $[\text{BF}_4\text{Bmim}]$  and  $[\text{PF}_6\text{Bmim}]$  ILs as structure directing agents in the synthesis of zeolites and comparing their results with those obtained for  $[\text{ClBmim}]$  and  $[\text{CH}_3\text{SO}_3\text{Bmim}]$  ILs.<sup>11</sup> In addition to the nature of the anion the concentration of the cosolvent (water or ethanol) is an issue to be considered.<sup>17–25</sup> At low concentration, water normally forms hydrogen bonds primarily with the anions but with the increase of its content hydrogen bonds with the cations are also formed.<sup>17,23,24</sup> When the water mole fraction is high enough ( $X_{\text{H}_2\text{O}} > 0.8$ ), a reduction of the cohesions between anions and cations is observed.<sup>14,17–25</sup> At these conditions, the original ion networks are no longer available and new water–cation/water–anion networks appeared.<sup>17–26</sup> This process induces changes in

Received: October 16, 2013

Revised: March 10, 2014

Published: March 10, 2014



several structural and dynamics properties of the liquid.<sup>14,27</sup> Generally the solubility of water in ILs increases with the temperature and the addition of ethanol enhances the solubility of water in alkyl imidazolium ions liquids with a large range of total miscibility in the triangular phase diagrams.<sup>28</sup> When the cosolvent is ethanol, the extension of the IL network disruption is less dramatic and larger ionic clusters appear in the IL/alcohol mixture due to the fact that ethanol molecules are much more homogeneously placed in the structure of the IL even at high ethanol concentrations.<sup>29–33</sup> These differences between cosolvents can be attributed to the lower dielectric constant of ethanol compared to that of water. Regarding the tertiary ILs/water/ethanol mixture, Wu et al.<sup>31</sup> concluded that ethanol molecules are capable of breaking the complexes cation...HOH...anion via cation–water and anion–water interactions. As a result, the addition of ethanol weakens the dissociation of ILs in water and the ILs network structure regains to a great extent.

Our aim in this work is two-fold. On one hand,  $[BF_4]Bmim]$  and  $[PF_6]Bmim]$  ILs were proposed and tested as possible structure directing agents for the synthesis of zeolites. On the other hand, an attempt on explaining the results in terms of the local structure of the water/IL and ethanol/IL mixtures is made. For this purpose, a quantum mechanical study of  $[XBmim]/$ cosolvent was carried out. Danten et al.<sup>34</sup> studied the local structure of water in ILs on the basis of IR spectroscopy and quantum chemical calculations and concluded that the local organization between ionic species in ILs is preliminary governed by electrostatic interactions. In this study was also claimed the necessity of considering the cation–anion pair dimer in quantum chemistry calculations as the minimal entity representative of the polar network of ILs, especially when the local structure is investigated. This need comes from the fact that the nonadditive interactions play a determining role in the description of ILs systems. For this reason and bearing in mind the experimental conditions, monomeric and dimeric ILs aggregates interacting with water or ethanol were considered. In the study, the unchanging IL  $[Bmim]^+$  cation and a variety of anions were considered ( $X \equiv Cl^-, BF_4^-, PF_6^-$  or  $CH_3SO_3^-$ ). As a cosolvent, water or ethanol was selected. The quantum chemical results of  $[XBmim]$  ILs interacting with water or ethanol could give a quite wide framework of analysis. Within it, the discussion on the similarities and differences among the two types of cosolvents and the relation between the structure of the clusters and the multiple factors defining the interactions among the  $[XBmim]$  IL and the cosolvent were focused. Undoubtedly, considering only cosolvent-ILs interactions as a representative of the local arrangement existing in ILs/cosolvent mixtures is an oversimplified image of the system under study. However, such an approach justified by the gain in computational resources will allow us to have a first idea about the main differences in the local structure of ILs + cosolvent and the consequences derived from them.

## ■ EXPERIMENTAL SECTION: ZEOLITE SYNTHESIS AND CHARACTERIZATION

In a typical synthesis, the Al precursor, IL template, and the base were dissolved in water in molar ratios corresponding to  $SiO_2/Al_2O_3/NaOH/IL/H_2O$  of 0.12:0.034:0.031:0.023:3.73 and then heated until the temperature reached 35 °C. Once the temperature was attained, the Si precursor, tetraethoxy silane (TEOS), was added and the solution was aged at this temperature for 4 h. Ethanol liberated from TEOS during the

hydrolysis stage together with water were considered as cosolvents and responsible for the IL/cosolvent interaction. After the aging period, a hydrothermal synthesis was performed in a stainless steel autoclave at 180 °C during 5 days. The resulted solid was then filtered, washed abundantly with ethanol, and dried at room temperature. Four templates were considered in these conditions:  $[XBmim]$ , where X was  $Cl^-$ ,  $BF_4^-$ ,  $PF_6^-$ , or  $CH_3SO_3^-$ .

The solids were submitted to the X-ray diffraction analysis performed on an X'Pert Pro PANalytical diffractometer. Diffraction patterns were recorded with CuKa radiation (40 mA, 45 kV) over 10 to 80° 2θ range of recorded by a position-sensitive detector using a step size of 0.05° and a step time of 80 s.

## ■ COMPUTATIONAL METHODS

Because monomeric  $[XBmim]$  and dimeric  $[XBmim]_2$  aggregates interacting with water or ethanol were considered and the large number of intermolecular degrees of freedom present in this type of clusters, it was necessary to find a suitable quantum chemical computational level to maintain within reasonable limits the computational cost. For this reason and bearing in mind the bibliography, the hybrid DFT method B3LYP<sup>35,36</sup> along with the 6-31++g(d,p) basis sets were selected. Quantum mechanics optimizations of  $[XBmim]$ ,  $[XBmim] + H_2O$ ,  $[XBmim] + EtOH$ ,  $[XBmim]_2$ ,  $[XBmim]_2 + H_2O$ , and  $[XBmim]_2 + EtOH$  aggregates (X being  $Cl^-$ ,  $BF_4^-$ ,  $PF_6^-$ , and  $CH_3SO_3^-$  anions) were carried out. At this point, it is worth pointing out that the complexity of the multidimensional energy surfaces precluded the determination of all the minima. Although many possible orientations for each cluster were explored, only the two most stable aggregates for  $[XBmim] + H_2O$ ,  $[XBmim] + EtOH$ ,  $[XBmim]_2$ ,  $[XBmim]_2 + H_2O$ , and  $[XBmim]_2 + EtOH$  species are presented. To carry out this selection the following procedure was performed: (i) Car–Parrinello molecular dynamics simulations of the clusters in gas phase at 350 K were run. This was done just as a source of initial configurations for lately ab initio optimizations. Therefore, the pseudopotentials were taken from the bibliography and their reliability was not tested in advance. (ii) Single point energy calculations of structures extracted from the trajectories were computed at B3LYP/6-31g level; (iii) the most stable clusters were optimized at B3LYP/6-31++g(d,p) level (B3LYP/6-31+g(d) level for the  $[XBmim]_2 +$  cosolvent clusters); and (iv) once this was done, the anions in the structures were exchanged and a new optimization was performed. This supplied a new source of initial configurations.

The largest clusters ( $[XBmim]_2 +$  cosolvent) were optimized at lower basis set quality, that is, 6-31+g(d). The differences between these two basis sets were negligible at both structure (tenths of angstroms) and energy (tenths of kcal/mol). In all cases, fully optimized structures were characterized by computing second energy derivatives. Bearing in mind the importance of accurate energy calculations for a study bases on interactions energies and for the sake of consistency, single point calculations with 6-31++g(d,p) basis sets on the optimized  $[XBmim]_2 +$  cosolvent structures were performed.<sup>37</sup> Computations were carried out by the Gaussian03 program.<sup>37</sup>

## ■ RESULTS AND DISCUSSION

The corresponding zeolite structures as a function of the ILs anion variation are presented in the Figure 1.

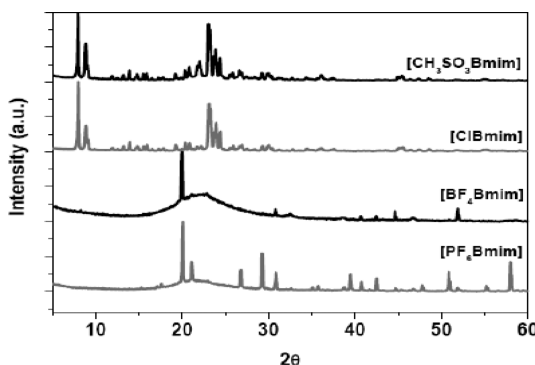


**Figure 1.** XR Diffractograms of the products derived from the synthesis using [XBmim] as a template (X being  $\text{Cl}^-$ ,  $\text{BF}_4^-$ ,  $\text{PF}_6^-$  and  $\text{CH}_3\text{SO}_3^-$ ).

The use of  $[\text{ClBmim}]$  and  $[\text{CH}_3\text{SO}_3\text{Bmim}]$  ILs as templates, as reported earlier,<sup>10</sup> led to the formation of MFI and BEA type zeolites with chemical composition corresponding to  $\text{Na}_{4.4}[\text{Al}_{4.5}\text{Si}_{9.1}\text{O}_{19.2}]$  and zeolite framework compensation by the  $\text{Na}^+$  cation. The [XBmim] content for both composites varies from 3.7 wt % for  $[\text{ClBmim}]$  to 4 wt % for  $[\text{CH}_3\text{SO}_3\text{Bmim}]$ . On the contrary,  $[\text{BF}_4\text{Bmim}]$  and  $[\text{PF}_6\text{Bmim}]$  ILs did not succeed in organizing the Si-Al network into a zeolite structure. The XRD pattern indicated the formation of amorphous phase mixed with the corresponding  $\text{NaBF}_4$  and  $\text{NaPF}_6$  salts. Those results suggested that the template function depends indirectly on the nature of the anion (resulting to be the element of dissimilarity) and on its induced properties on the behavior of the ionic liquid itself. On the other side, as reported previously<sup>10</sup> the formation of the zeolite structure also depends on the [XBmim] nearest chemical environment and especially on its interaction with the cosolvent (water and/or ethanol).

To characterize the preferred interaction sites and the relative position of cation-anion and cation-anion-cosolvent,  $[\text{XBmim}]$ ,  $[\text{XBmim}] + \text{H}_2\text{O}$ ,  $[\text{XBmim}] + \text{EtOH}$ ,  $[\text{XBmim}]_2$ ,  $[\text{XBmim}]_2 + \text{H}_2\text{O}$  and  $[\text{XBmim}]_2 + \text{EtOH}$  aggregates (X being  $\text{Cl}^-$ ,  $\text{BF}_4^-$ ,  $\text{PF}_6^-$  and  $\text{CH}_3\text{SO}_3^-$  anions) were analyzed.

The components of the ILs were collected in Figure 2. An individual analysis of them indicates that the H atom bonded to the C atom between the two N atoms in the  $[\text{Bmim}]^+$  cation is the most acid H atom in the ring (labeled as  $\text{H}_2$  for now on) and in principle would be the preferred interaction site for both

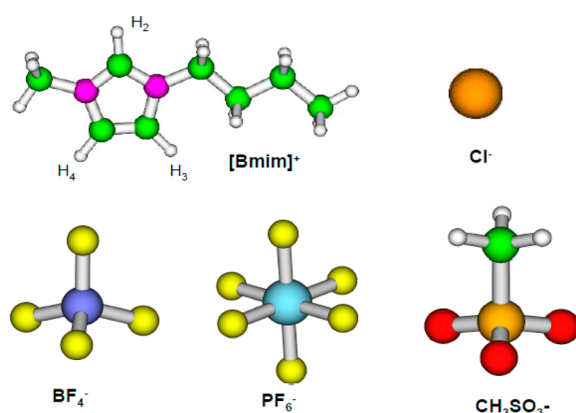


**Figure 2.** Structures for the  $[\text{Bmim}]^+$ ,  $\text{Cl}^-$ ,  $\text{BF}_4^-$ ,  $\text{PF}_6^-$  and  $\text{CH}_3\text{SO}_3^-$  ionic species optimized at B3LYP/6-31++g(d,p) level.

anions and cosolvents.<sup>38–41</sup> The  $\text{Cl}^-$  anion is monatomic.  $\text{BF}_4^-$  and  $\text{PF}_6^-$  anions are nonpolar and symmetric species from the interaction point of view.  $\text{CH}_3\text{SO}_3^-$  anion is polar and nonsymmetric for the interaction with  $[\text{Bmim}]^+$  cation, water, or ethanol. These inherent features will be relevant in the analysis of the final structures here studied.

## ■ [XBmim] CLUSTERS

The optimized structures along with their corresponding interaction energies for the [XBmim] monomers were collected in Figure 3.

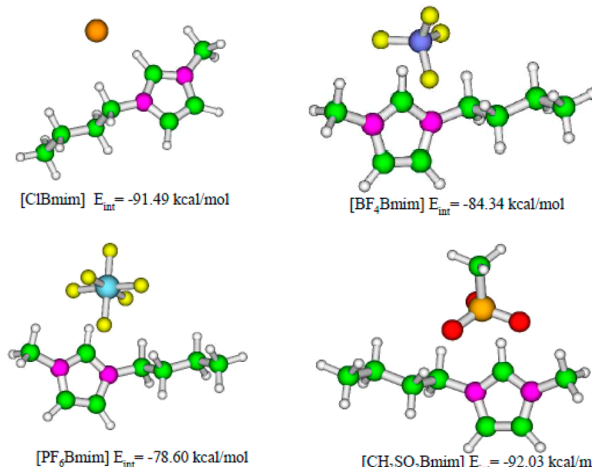


**Figure 3.** [XBmim] clusters (X being  $\text{Cl}^-$ ,  $\text{BF}_4^-$ ,  $\text{PF}_6^-$  and  $\text{CH}_3\text{SO}_3^-$ ) optimized at B3LYP/6-31++g(d,p) level along with their interaction energies in kcal/mol.

The [XBmim] ion pair formation was governed by the electrostatic interaction between the cation and the anion. Additionally, nonbonding interactions played a non-negligible role, the interaction between the anions and the acidic  $\text{H}_2$  being the most significant. However, the relative position of the cation versus the anion was also given by the interaction of the H atoms of the alkyl side chains with the anion. In the case of the  $\text{Cl}^-$  ion, the possibility of simultaneous multiple interactions with the alkyl imidazolium cation was partially restricted by its monatomic character and small size. A detailed analysis of the structure collected in Figure 3 indicated that the  $\text{C}_1-\text{H}_2-\text{Cl}$  angle was  $158.6^\circ$  allowing certain interaction with one of the H atoms of the first C atom in the butyl chain ( $\text{Cl}-\text{H}(\text{butyl})$  distance was  $2.64 \text{ \AA}$ ). The polyatomic character of the remaining anions along with their larger size allowed simultaneous interactions with the  $\text{H}_2$  atom and with the H atoms of the alkyl chains. The relative position of the anion versus the cation was different for the  $\text{Cl}^-$  ion from the  $\text{BF}_4^-$ ,  $\text{PF}_6^-$ , and  $\text{CH}_3\text{SO}_3^-$  species. While the former was located in the same plane of the ring, the latter ones were arranged over the ring. Experimental evidence of these differences were found using IR spectroscopy.<sup>41</sup> The interaction energies ( $E_{\text{int}}$ ) for the [XBmim] monomers were  $-91.49$ ,  $-84.34$ ,  $-78.60$ , and  $-92.03$  kcal/mol for  $\text{Cl}^-$ ,  $\text{BF}_4^-$ ,  $\text{PF}_6^-$ , and  $\text{CH}_3\text{SO}_3^-$  species, respectively. Globally, the structures and interaction energies were found in agreement with previous studies.<sup>34,42–49</sup>

## ■ [XBmim] + COSOLVENT CLUSTERS

When water and ethanol cosolvents were considered, two different arrangements were found. On one hand, the cosolvent

closer to the H<sub>2</sub> atom than the anion and, on the other hand, the anion closer to the H<sub>2</sub> atom of the ring than the cosolvent. For the four ILs, both situations were minima in their corresponding potential energy surfaces.

The optimized structures along with their corresponding interaction energies for the [XBmim] + H<sub>2</sub>O aggregates were collected in Figure 4.

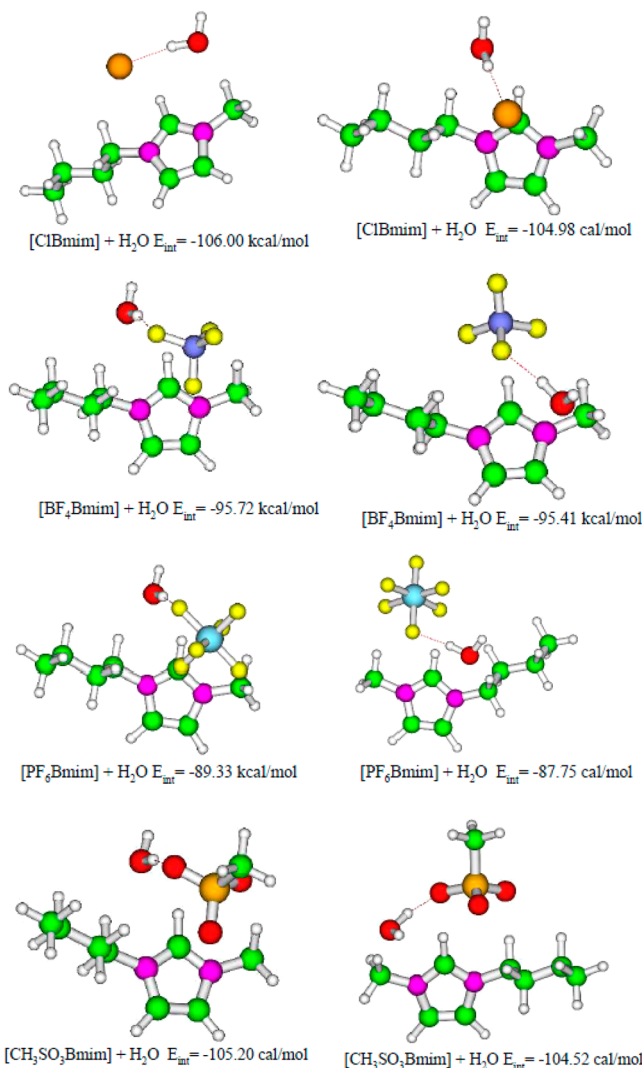


**Figure 4.** [XBmim] + H<sub>2</sub>O clusters (X being Cl<sup>-</sup>, BF<sub>4</sub><sup>-</sup>, PF<sub>6</sub><sup>-</sup>, and CH<sub>3</sub>SO<sub>3</sub><sup>-</sup>) optimized at B3LYP/6-31++g(d,p) level along with their interaction energies in kcal/mol.

In the case of the Cl<sup>-</sup> anion, the cluster with the anion closer to the ring than the water molecule was more stable by 1.02 kcal/mol. This aggregate was similar to the one without the water molecule. Although the water molecule was away from the cation, the water molecule also interacted with it. This way, it was located over the ring and interacted with a H atom of the methyl group. In the cluster with the water molecule closer to the ring ( $E_{\text{int}} = -104.98$  kcal/mol), there was also an interaction of the cosolvent molecule with the alkyl chain but with the butyl chain. In this minimum, the Cl<sup>-</sup> anion was located over the imidazolium ring whereas the water molecule was in plane with the ring. For the BF<sub>4</sub><sup>-</sup> anion, the most stable aggregate ( $E_{\text{int}} = -95.72$  kcal/mol) was the one with the water molecule closer to the ring whereas at only 0.32 kcal/mol, there

was another cluster with the anion closer to the imidazolium ring. In both structures, the BF<sub>4</sub><sup>-</sup> species was over the imidazolium plane. The water molecule was in the plane of the ring in the first aggregate but over this plane in the second one. The interaction of the anion and the water molecule with the H atoms of the alkyl chains fixed their relative positions with respect to the ring. When the PF<sub>6</sub><sup>-</sup> anion was considered, the most stable structure ( $E_{\text{int}} = -89.33$  kcal/mol) was the one with the water molecule closer to the ring and the PF<sub>6</sub><sup>-</sup> anion over the imidazolium plane. In this cluster, the H atoms of the butyl chain interacted with both the water molecule and the PF<sub>6</sub><sup>-</sup> anion. In the aggregate with the PF<sub>6</sub><sup>-</sup> anion closer to the ring ( $E_{\text{int}} = -87.75$  kcal/mol), two of the anion's F atoms simultaneously interacted with the H<sub>2</sub> atom, as a consequence the anion and the ring were roughly in the same plane whereas the water molecule was over the ring. The PF<sub>6</sub><sup>-</sup> anion also interacted with the methyl group as the water molecule did with the butyl group. For the CH<sub>3</sub>SO<sub>3</sub><sup>-</sup> anion, the most stable structure ( $E_{\text{int}} = -105.20$  kcal/mol) was the one with the water molecule closer to the ring and the CH<sub>3</sub>SO<sub>3</sub><sup>-</sup> anion over the [Bmim]<sup>+</sup> cation interacting with the H<sub>2</sub> atom and with the methyl group. A second structure similar in energy ( $E_{\text{int}} = -104.52$  kcal/mol) presented the CH<sub>3</sub>SO<sub>3</sub><sup>-</sup> anion closer to the ring than the water molecule. In this case, the CH<sub>3</sub>SO<sub>3</sub><sup>-</sup> anion was situated above the ring and the interaction of the water molecule with the [Bmim]<sup>+</sup> cation mainly occurred via the methyl group.

As expected, in all the structures the hydrogen bond between the water molecule and the anion was observed. The distance between the H of the water molecule and the anion (Cl, F or O atoms) entered in the interval [1.70–2.13] Å. The detailed description of the previous structures suggested that the water molecule interacted with both partners of the anion/cation couple even if on some occasions the interaction of water with the imidazolium ring did not present a specific hydrogen bond nature. Additionally to the primary stabilizing factors due to the electrostatic contribution and the hydrogen bond for the cation/anion/water system, the interaction between the H atoms of the alkyl chains with the anion and water molecule were responsible for the relative orientation of the side chains. As in the case of the monomers, the ion pair containing Cl<sup>-</sup> behaved differently from the other anions. The most stable situation was the one with Cl<sup>-</sup> close to the ring and coplanar with it whereas the BF<sub>4</sub><sup>-</sup>, PF<sub>6</sub><sup>-</sup>, and CH<sub>3</sub>SO<sub>3</sub><sup>-</sup> species preferred to be over the ring and away from it with the water molecule in a closer position. The analysis of the interaction energies indicated that Cl<sup>-</sup> and CH<sub>3</sub>SO<sub>3</sub><sup>-</sup> aggregates presented similar values (-106.00 and -105.20 kcal/mol, respectively) whereas the clusters with BF<sub>4</sub><sup>-</sup> and PF<sub>6</sub><sup>-</sup> species were less stable (-95.72 and -89.33 kcal/mol, respectively). The trend followed by the monomers was kept when the interaction with a water molecule was considered.

The optimized structures along with their corresponding interaction energies for the [XBmim] + EtOH aggregates were collected in Figure 5.

In the case of the Cl<sup>-</sup> ion, similarly to that of water as a cosolvent, the cluster with the Cl<sup>-</sup> closer to the imidazolium ring than the ethanol molecule was more stable by 0.85 kcal/mol. Both the Cl<sup>-</sup> and the ethanol molecule were in the plane of the imidazolium ring. Different behavior was found for the BF<sub>4</sub><sup>-</sup> anion. The structure with the ethanol molecule closer to the ring was almost as stable as (-94.96 kcal/mol versus -94.76 kcal/mol) that with two F atoms interacting with the

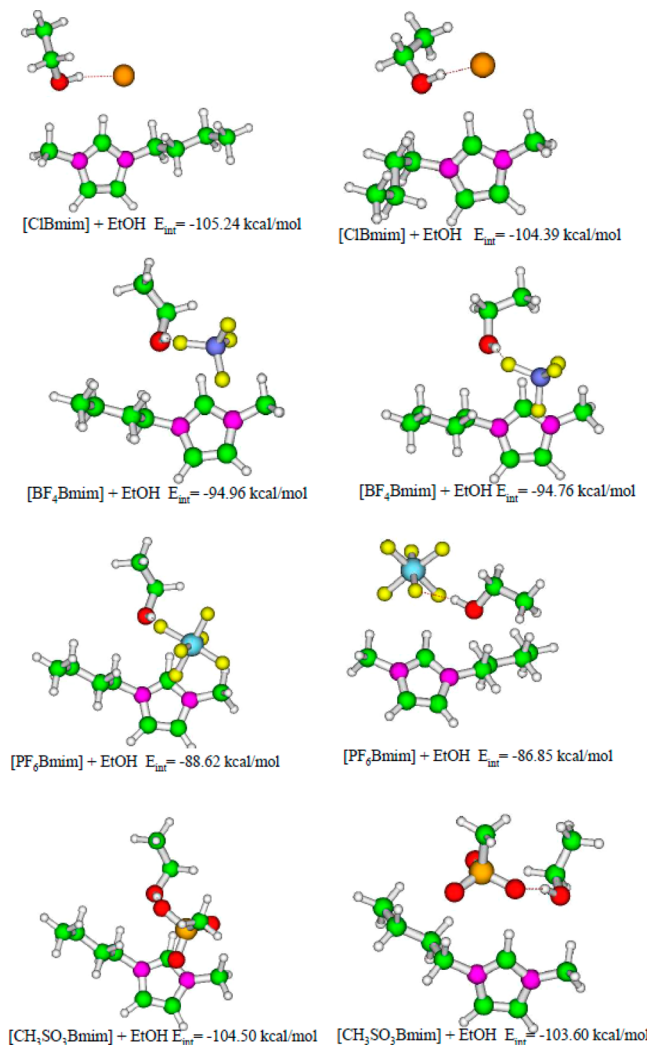


**Figure 5.**  $[XBmim]$  + EtOH clusters ( $X$  being  $\text{Cl}^-$ ,  $\text{BF}_4^-$ ,  $\text{PF}_6^-$  and  $\text{CH}_3\text{SO}_3^-$ ) optimized at B3LYP/6-31++g(d,p) level along with their interaction energies in kcal/mol.

$\text{H}_2$  atom. The  $\text{BF}_4^-$  anion and the ethanol molecule were located over the imidazolium plane and in the same plane, respectively. In the cluster with the  $\text{PF}_6^-$  anion, the most stable situation appeared when the ethanol was adjacent to the  $\text{H}_2$  atom ( $E_{\text{int}} = -88.62$  kcal/mol). The  $\text{PF}_6^-$  anion was located over the imidazolium plane contrary to the ethanol in plane position. The hydrogen bond between several F atoms and the  $\text{H}_2$  atom led to decrease the stability of the cluster ( $E_{\text{int}} = -86.85$  kcal/mol). The anion's larger size allowed also the

interaction with both alkyl chains. In this case, the ethanol molecule was coplanar with the imidazolium ring whereas the  $\text{PF}_6^-$  anion was not included in this plane. Regarding the aggregate with  $\text{CH}_3\text{SO}_3^-$  species, the most stable ( $E_{\text{int}} = -104.50$  kcal/mol) was the one with the ethanol molecule closer and coplanar to the ring. In the second minimum ( $E_{\text{int}} = -103.60$  kcal/mol), the relative positions of the  $\text{CH}_3\text{SO}_3^-$  anion and ethanol molecule were exchanged and the anion was in the plane of the ring whereas the cosolvent molecule was over it.

No matter the anion in the aggregate, the interaction between the ethanol and the anion occurred via hydrogen bond. The distance between the H of the ethanol molecule and the anion was similar to that found for the water molecule ([1.73–2.15] Å versus [1.70–2.13] Å). In all cases, the  $\text{CH}_3-\text{CH}_2-$  chain of the ethanol was orientated apart from either the cation or the anion. Like in the case of the water molecule, the cluster with  $\text{Cl}^-$  anion behaved in a different way from the rest of the species and the interaction energies for the  $\text{Cl}^-$  and  $\text{CH}_3\text{SO}_3^-$  species were very similar and larger than those for the  $\text{BF}_4^-$  and  $\text{PF}_6^-$  ones. What's more, the  $E_{\text{int}}$  for  $[XBmim]$  + water or ethanol appeared to depend on the anion but not on the cosolvent. For an easy comparison, Table 1 recollects the  $E_{\text{int}}$  for the most stable clusters.

## ■ $[XBmim]_2$ CLUSTERS

The lowest energy minimum structures for the  $[XBmim]_2$  ion pair dimers along with their interaction energies were shown in Figure 6.

It can be seen that dimers presented a different structure than just the sum of monomers. Cations and anions were organized as a result of a compromise between attractive contributions (anion–cation) and repulsive interactions (anion–anion and cation–cation). Regardless the specific details of each structure, they can be defined according to (1) the relative position and orientation of the imidazolium rings to each other and (2) the relative position of the anions with respect to the imidazolium rings. To illustrate the structures, two angles were computed; the angle between the planes containing the rings ( $a1$ ) and the angle between the  $((C_2 + C_3)/2, C_1)$  vectors of each ring ( $a2$ ). The angle  $a1$  gave information about the relative position of the rings. This way, a value of 180 or  $0^\circ$  implied parallel rings whereas a value equal to  $90^\circ$  meant perpendicular rings. The angle  $a2$  gave information about the orientation of the rings, in particular the spinning of the rings one to another. A value of  $a2$  close to  $0^\circ$  implied the rings orientated toward the same side whereas  $a2$  equal to  $180$  or  $90^\circ$  meant opposite or perpendicular orientation, respectively. Chart 1 showed an

**Table 1. Interaction Energies ( $E_{\text{int}}$ ) for the Most Stable  $[XBmim]$ ,  $[XBmim]$  + Cosolvent,  $[XBmim]_2$ , and  $[XBmim]_2$  + Cosolvent Clusters Optimized at B3LYP/6-31++g(d,p) Level (B3LYP/631+g(d) Level for  $[XBmim]_2$  + Cosolvent Aggregates)<sup>a</sup>**

| X                                  | $\text{Cl}^-$     | $\text{BF}_4^-$   | $\text{PF}_6^-$   | $\text{CH}_3\text{SO}_3^-$ |
|------------------------------------|-------------------|-------------------|-------------------|----------------------------|
| $[XBmim]$                          | -91.49            | -84.34            | -78.60            | -92.03                     |
| $[XBmim]$ + $\text{H}_2\text{O}$   | -106.00           | -95.72            | -89.33            | -105.20                    |
| $[XBmim]$ + EtOH                   | -105.24           | -94.96            | -88.62            | -104.50                    |
| $[XBmim]_2$                        | -204.30           | -189.63           | -178.44           | -206.67                    |
| $[XBmim]_2$ + $\text{H}_2\text{O}$ | -218.47 (-218.41) | -198.57 (-198.55) | -188.40 (-188.24) | -219.00 (-219.05)          |
| $[XBmim]_2$ + EtOH                 | -217.46 (-217.30) | -199.95 (-200.12) | -186.81 (-187.10) | -219.52 (-220.38)          |

<sup>a</sup>Single point energy calculations using 6-31++g(d,p) basis sets for the  $[XBmim]_2$  + cosolvent structures optimized at B3LYP/6-31+g(d) level are given in parentheses. All values are given in kcal/mol.

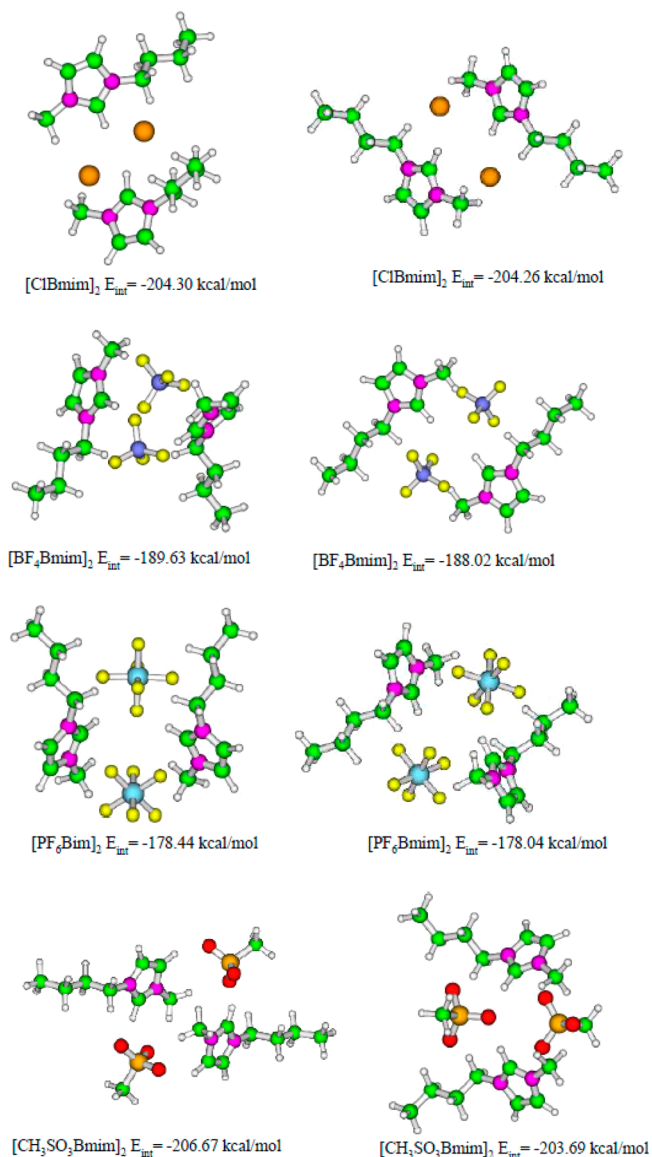


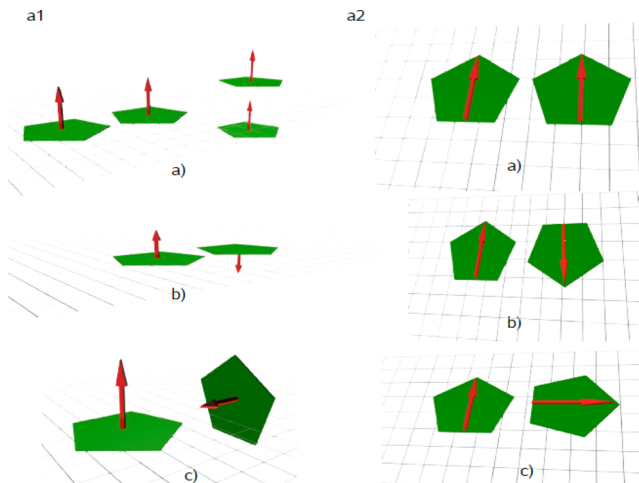
**Figure 6.**  $[XBmim]_2$  clusters ( $X$  being  $\text{Cl}^-$ ,  $\text{BF}_4^-$ ,  $\text{PF}_6^-$  and  $\text{CH}_3\text{SO}_3^-$ ) optimized at B3LYP/6-31++g(d,p) level along with their interaction energies in kcal/mol.

outline of the parallel and perpendicular position and orientation of the rings on the basis of  $a1$  and  $a2$  angles.

The position of the anion species respect of the  $[\text{Bmim}]^+$  cation was defined in terms of being either coplanar with the rings or over them. Although the relative position of the two rings and the orientation of their alkyl chains can not run in parallel, this information has not been reported just for simplicity. For a better comparison of the dimers, the values of  $a1$  and  $a2$  angles for the most stable dimers were collected in Table 2.

A detailed analysis of Figure 6 indicated that in the case of the  $\text{Cl}^-$  anion, the most stable dimer ( $E_{\text{int}} = -204.30 \text{ kcal/mol}$ ) had the rings in an intermediate situation between being parallel or perpendicular ( $a1 = 135.9^\circ$  and  $a2 = 144.8^\circ$ ) with each  $\text{Cl}^-$  anion coplanar with one imidazolium ring. The  $\text{Cl}-\text{Cl}$  distance was  $4.48 \text{ \AA}$ . This short distance between anions can only be understood when the cation screening is considered. A second minimum ( $E_{\text{int}} = -204.26 \text{ kcal/mol}$ ) presented the rings in a parallel ( $a1 = 180.0^\circ$ ) and opposite arrangement ( $a2$

**Chart 1. Outline of the Imidazolium Rings Position (left)<sup>a</sup> and Orientation (left)<sup>b</sup>**



<sup>a</sup>(a,b) The parallel arrangement, which means  $a1 = 180$  or  $0^\circ$  and (c) indicates the perpendicular position. <sup>b</sup>(a) The rings orientated to the same side, (b) the rings orientated opposite, and (c) the perpendicular arrangement.

$= 180.0^\circ$ ) with each  $\text{Cl}^-$  anion coplanar with one ring. These two minima close in energy revealed that there was not one unique interaction pattern in these clusters, thus resulting in different scenarios where the cosolvent molecules can interact with both anions and cations.

In the case of the  $\text{BF}_4^-$  anion, the most stable aggregate ( $E_{\text{int}} = -189.63 \text{ kcal/mol}$ ) presented the imidazolium rings at  $a1 = 63.8^\circ$  with a perpendicular orientation ( $a2 = 91.6^\circ$ ). One of the  $\text{BF}_4^-$  anion was above the rings whereas the other  $\text{BF}_4^-$  anion was between them. The  $\text{B}-\text{B}$  distance was  $5.56 \text{ \AA}$ . In a second minimum ( $E_{\text{int}} = -188.02 \text{ kcal/mol}$ ) the rings were parallel ( $a1 = 180.0^\circ$ ) and opposite ( $a2 = 180.0^\circ$ ) to each other. Both  $\text{BF}_4^-$  anions were situated above the rings interacting not only with them but with the side chains as well. The distance between  $\text{B}$  atoms of each anion was shorter ( $5.22 \text{ \AA}$ ) than in the first case.

The analysis of the dimers with the  $\text{PF}_6^-$  anions revealed that the most stable structure ( $E_{\text{int}} = -178.44 \text{ kcal/mol}$ ) presented the rings perpendicular to each other ( $a1 = 95.2^\circ$  and  $a2 = 94.5^\circ$ ). Similar to  $\text{BF}_4^-$  position, one of the  $\text{PF}_6^-$  anions stayed above the imidazolium rings while the other  $\text{PF}_6^-$  anion was between them. The  $\text{P}-\text{P}$  distance appeared to be  $6.18 \text{ \AA}$ . In a second minimum ( $E_{\text{int}} = -178.04 \text{ kcal/mol}$ ), the imidazolium rings were almost parallel ( $a1 = 23.8^\circ$ ) and slightly rotated ( $a2 = 159.6^\circ$ ) with each  $\text{PF}_6^-$  anion located above an imidazolium ring.

When the dimers with the  $\text{CH}_3\text{SO}_3^-$  anions were considered, the structure with the rings almost parallel ( $a1 = 8.4^\circ$ ) was more stable by  $\sim 3 \text{ kcal/mol}$ . The  $\text{CH}_3\text{SO}_3^-$  anions were above and below the imidazolium rings giving rise to a new interaction not seen so far, namely the interaction between one of the  $\text{O}$  atoms of the  $\text{CH}_3\text{SO}_3^-$  species and the  $\text{H}_3$  atom of the ring (see Figure 2 for detail). This interaction was possible because the rings are turned ( $a2 = 177.1^\circ$ ) to each other. Although this  $\text{H}$  atom was less acidic than the  $\text{H}_2$  atom, it played a significant role in the description of this structure. Both anions were rather separated, the  $\text{S}-\text{S}$  distance being  $7.73 \text{ \AA}$ . A second minimum ( $E_{\text{int}} = -203.0 \text{ kcal/mol}$ ) considered the rings almost perpendicular ( $a1 = 107.0^\circ$  and  $a2 = 104.8^\circ$ ) with one  $\text{CH}_3\text{SO}_3^-$  anion closer to the rings than to its homologue,

**Table 2.** Angles That Show the Position (a1) and Orientation (a2) of the Imidazolium Rings for the Most Stable  $[XBmim]_2$  and  $[XBmim]_2 + \text{Cosolvent Clusters}^a$

| X                                      | $\text{Cl}^-$ | $\text{BF}_4^-$ | $\text{PF}_6^-$ | $\text{CH}_3\text{SO}_3^-$ |
|--|---------------|-----------------|-----------------|----------------------------|
| $[XBmim]_2$ a1/a2                      | 135.9/144.8   | 63.8/91.6       | 95.2/94.5       | 8.4/177.1                  |
| $[XBmim]_2 + \text{H}_2\text{O}$ a1/a2 | 141.9/156.1   | 97.6/92.5       | 6.0/167.5       | 9.1/155.6                  |
| $[XBmim]_2 + \text{EtOH}$ a1/a2        | 18.5/160.6    | 148.3/135.7     | 6.4/171.6       | 174.9/122.2                |

<sup>a</sup>All values are in degrees.

which is the first  $\text{CH}_3\text{SO}_3^-$  anion being above the rings and the second between them. In this case, the interaction between the anions and the ring's H<sub>3</sub> atom was not observed and the S–S distance was clearly shorter (5.92 Å).

All those results pointed again to the significant role of the nonbonding interactions and the relative position of each species, together with the primary electrostatic factors responsible for the dimers stabilization. For a given anion, the two minima considered in every case were very close in energy but different in structures. As for the previous aggregates ( $[XBmim]$  and  $[XBmim] + \text{cosolvent}$ ), the interaction energies for  $\text{Cl}^-$  and  $\text{CH}_3\text{SO}_3^-$  dimers were closer in values and stability than those for  $\text{BF}_4^-$  and  $\text{PF}_6^-$  species (see Table 1 for details).

## ■ $[XBmim]_2 + \text{COSOLVENT CLUSTERS}$

When a cosolvent molecule was added to the dimers different situations were obtained. The detailed description of these structures was involved due to the large size of the systems and the large number of interactions sites. For the sake of simplicity and taking into account the comparative purpose of this study, only the main differences among the minima will be discussed. The description of the  $[XBmim]_2 + \text{cosolvent}$  structures was based on the relative position and orientation of the imidazolium rings (a1 and a2 angles) and the position of the anions with respect to the imidazolium rings. The values of a1 and a2 for the most stable clusters were collected in Table 2.

The minima for  $[XBmim]_2 + \text{H}_2\text{O}$  aggregates along with their interaction energies were collected in Figure 7.

In the case of the  $\text{Cl}^-$  anion, the water molecule was bonded to both anions simultaneously via hydrogen bond forming a nearly symmetric structure  $\text{Cl}\cdots\text{H}–\text{O}–\text{H}\cdots\text{Cl}$ , in which each H atom of the water molecule interacted with one  $\text{Cl}^-$  anion. The most stable situation ( $E_{\text{int}} = -218.47 \text{ kcal/mol}$ ) corresponded to the imidazolium rings in an intermediate position between being parallel or perpendicular (a1 = 141.9°) and slightly turned (a2 = 156.1°) with each  $\text{Cl}^-$  anion coplanar with an imidazolium ring. The water molecule was further from the acidic atoms than the  $\text{Cl}^-$  anions. The Cl–Cl distance of 4.37 Å was close to the value found for the  $[\text{ClBmim}]_2$  dimer (4.48 Å). A second minimum ( $E_{\text{int}} = -217.20 \text{ kcal/mol}$ ) with the rings positioned at a1 = 64.3° and orientated at a2 = 116.8° was obtained. In this case, the first  $\text{Cl}^-$  anion and the water molecule were over an imidazolium ring while the second  $\text{Cl}^-$  anion was in the plane of the other imidazolium ring close to the alkyl chains. A comparison of the two minima indicated that the relative position of the water molecules regards to the anions was kept but it differed with respect to the cations.

In the case of the  $\text{BF}_4^-$  anion, the water molecule was located between the anions forming hydrogen bonds with both, in such a way that each H atom of the water molecule interacted with a F atom of different anions. The most stable cluster ( $E_{\text{int}} = -198.57 \text{ kcal/mol}$ ) had the rings rather perpendicular to each other (a1 = 97.6° and a2 = 92.5°) with one  $\text{BF}_4^-$  anion over the plane of an imidazolium ring and the other  $\text{BF}_4^-$  anion together

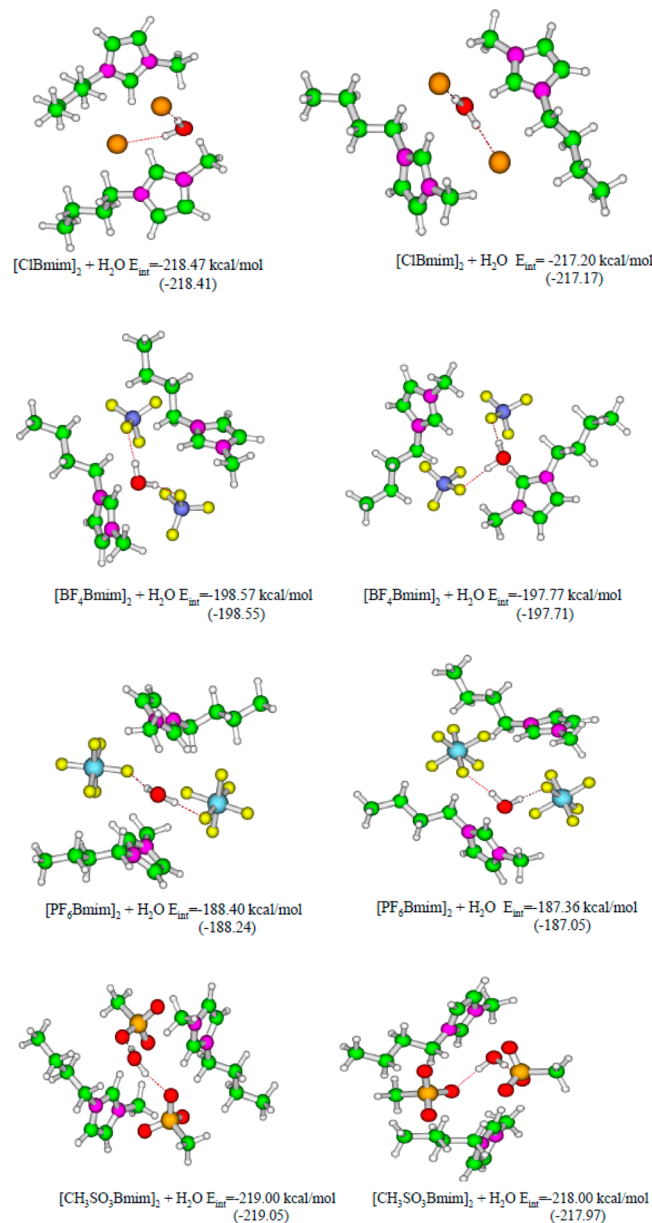


**Figure 7.**  $[XBmim]_2 + \text{H}_2\text{O}$  clusters (X being  $\text{Cl}^-$ ,  $\text{BF}_4^-$ ,  $\text{PF}_6^-$ , and  $\text{CH}_3\text{SO}_3^-$ ) optimized at B3LYP/6-31+g(d) level along with their interaction energies in kcal/mol. Single point energy calculations using 6-31+g(d,p) basis sets at the optimized BL3LYP/6-31+g\* structures are presented in parentheses.

with the water molecule in plane with the other ring. The B–B distance was similar to the calculated for the  $[\text{BF}_4\text{Bmim}]_2$  dimer (5.34 versus 5.56 Å). A second structure ( $E_{\text{int}} = -197.77 \text{ kcal/mol}$ ) presented the rings at a1 = 34.8° and a2 = 175.1°. The  $\text{BF}_4^-$  anions interacted with both the H<sub>2</sub> atoms and the

alkyl chains with each  $\text{BF}_4^-$  anion in the plane of its corresponding imidazolium ring.

Similar to the  $\text{BF}_4^-$ , the water molecule was located between the  $\text{PF}_6^-$  anions forming hydrogen bonds with them. The most stable situation ( $E_{\text{int}} = -188.40$  kcal/mol) presented the  $\text{PF}_6^-$  anions closer to the  $\text{H}_2$  atoms than the water molecule. One of the  $\text{PF}_6^-$  species interacted with the  $\text{H}_3$  atom of one of the rings, a scenario only given when the rings were almost parallel ( $a_1 = 6.0^\circ$ ) and opposite orientated ( $a_2 = 167.5^\circ$ ) with the butyl chains opposite to each other. Each  $\text{PF}_6^-$  anion was in the plane of its ring and over the other ring, simultaneously. The P–P distance was 6.42 Å. A second minimum very close in energy ( $E_{\text{int}} = -187.36$  kcal/mol) with the absence of F–H<sub>3</sub> interaction and the water molecule closer to one of the H<sub>2</sub> atoms was found. In this case, the rings were roughly perpendicular ( $a_1 = 76.8^\circ$  and  $a_2 = 78.1^\circ$ ) with the  $\text{PF}_6^-$  anions above the rings in parallel planes.

In the case of  $\text{CH}_3\text{SO}_3^-$  anions, the water molecule was located between the anions forming hydrogen bonds with them in such a way that each H atom of the water molecule interacted with an O atom of different anions. Among the different minima found, the most stable ( $E_{\text{int}} = -219.00$  kcal/mol) was that presenting the imidazolium rings almost parallel ( $a_1 = 9.1^\circ$ ) and rotated with  $a_2 = 154.6^\circ$ . The  $\text{CH}_3\text{SO}_3^-$  species were closer to the H<sub>2</sub> atom of the rings than the water molecule giving rise to an arrangement in which each  $\text{CH}_3\text{SO}_3^-$  anion was coplanar to one ring and over the other one. The calculated S–S distance of 4.90 Å was shorter than that obtained in the dimers (7.73 and 5.92 Å). A second minimum like the first one ( $E_{\text{int}} = -218.00$  kcal/mol) presented the rings almost parallel ( $a_1 = 170.1^\circ$ ) and a bit rotated ( $a_2 = 155.6^\circ$ ) but with the water molecule closer to the H<sub>2</sub> atom of one of them. One of the  $\text{CH}_3\text{SO}_3^-$  anions was above both imidazolium rings and the other anion between them.

The analysis of the  $[\text{XBmim}]_2 + \text{H}_2\text{O}$  species revealed that the water molecule did not change the relative order of interaction energies observed in the dimers. In all cases, the water molecule interacted with both anions simultaneously playing the role of a double proton donor. This was already observed for the  $\text{Cl}^-$ ,  $\text{BF}_4^-$ , and  $\text{PF}_6^-$  anions<sup>16,32,36,41,50,51</sup> but as far as we know it has not been confirmed for the  $\text{CH}_3\text{SO}_3^-$  species yet. It is clear that the correlation between the anions and the water molecule was more significant than that for the cations and the water species. The similarities in interaction energies showed by the different minima analyzed for each anion evidenced that water–cation network can not be well established.

The lowest energy minimum structures for the  $[\text{XBmim}]_2 + \text{EtOH}$  clusters are shown in Figure 8.

Opposite to the water behavior, the ethanol molecule could not interact with both anions simultaneously. The topology of the ethanol molecule precluded the possibility of playing the role of a double proton donor. In the case of the  $\text{Cl}^-$  anion, the most stable  $[\text{ClBmim}]_2 + \text{EtOH}$  cluster ( $E_{\text{int}} = -217.46$  kcal/mol) presented the rings almost parallel ( $a_1 = 18.5^\circ$ ) and oppositely orientated ( $a_2 = 160.6^\circ$ ). Each  $\text{Cl}^-$  anion and the ethanol molecule were in the plane of one of the rings. The ethanol molecule interacted only with one  $\text{Cl}^-$  anion and with the H<sub>3</sub> atom of one of the rings without any specific interaction between the alkyl chains and the ethanol molecule. This type of interaction between the cosolvent and the H<sub>3</sub> atom already appeared in the  $[\text{PF}_6\text{Bmim}]_2 + \text{H}_2\text{O}$  cluster. The calculated Cl–Cl distance of 6.80 Å was in agreement with the

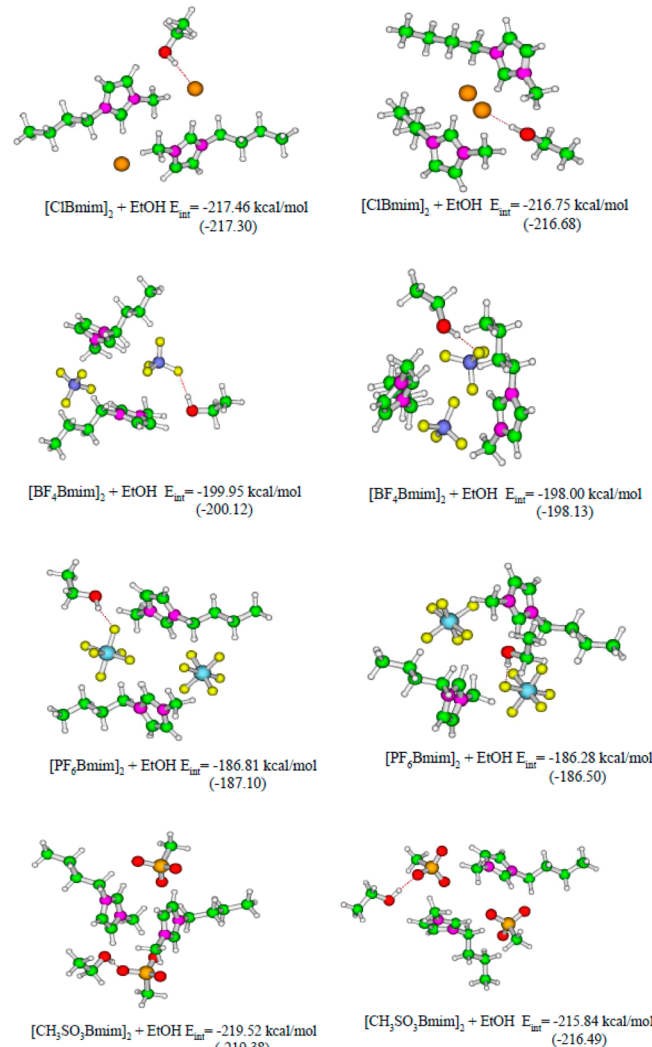


**Figure 8.**  $[\text{XBmim}]_2 + \text{EtOH}$  clusters (X being  $\text{Cl}^-$ ,  $\text{BF}_4^-$ ,  $\text{PF}_6^-$ , and  $\text{CH}_3\text{SO}_3^-$ ) optimized at B3LYP/6-31+g(p) level along with their interaction energies in kcal/mol. Single point energy calculations using 6-31+g(d,p) basis sets at the optimized BL3LYP/6-31+g(d) structures are presented in parentheses.

simultaneous interaction of one  $\text{Cl}^-$  anion with the H<sub>2</sub> atom of one ring and the H<sub>3</sub> atom of the other imidazolium ring. A second energy minimum ( $E_{\text{int}} = -216.75$  kcal/mol) described the rings positions almost in a parallel position and oppositely orientated ( $a_1 = 177.3^\circ$  and  $a_2 = 160.6^\circ$ ). Each  $\text{Cl}^-$  anion was in the plane of an imidazolium ring and over the other one. The ethanol molecule interacted with one of the  $\text{Cl}^-$  anions and with the methyl groups of both rings. Although only separated by 0.71 kcal/mol, the structures of both minima were very different.

For the  $[\text{BF}_4\text{Bmim}]_2 + \text{EtOH}$  species, the cosolvent molecule only interacted with one of the  $\text{BF}_4^-$  anions for all the minima studied. In the most stable cluster ( $E_{\text{int}} = -199.95$  kcal/mol), the rings were positioned at  $a_1 = 148.3^\circ$  to each other and rotated ( $a_2 = 135.7^\circ$ ). One  $\text{BF}_4^-$  species was in the plane of both imidazolium rings and the other  $\text{BF}_4^-$  species over them. The ethanol molecule interacted with one of the  $\text{BF}_4^-$  anions with the H<sub>3</sub> atom of one of the rings and with the methyl group of the same ring. The B–B distance was 5.89 Å. A second minimum ( $E_{\text{int}} = -198.00$  kcal/mol) presented the rings almost perpendicular ( $a_1 = 112.1^\circ$  and  $a_2 = 80.6^\circ$ ) and each  $\text{BF}_4^-$

anion was in the plane of one ring and over the other one, simultaneously. The ethanol molecule interacted with one of the  $\text{BF}_4^-$  anions with the  $\text{H}_2$  atom of one of the rings and with the methyl chain of that ring.

For the  $[\text{PF}_6\text{Bmim}]_2 + \text{EtOH}$  aggregates, the most stable cluster ( $E_{\text{int}} = -186.81 \text{ kcal/mol}$ ) accounted for the interaction of the anions with the  $\text{H}_2$  atoms of the rings and with the alkyl chains. This was possible because each  $\text{PF}_6^-$  species was located in the plane of one imidazolium ring and over the other one. In turn, the ethanol molecule interacted with one of the  $\text{PF}_6^-$  anions with the  $\text{H}_3$  atom of one of the rings and with its methyl chain. The rings were almost parallel ( $a1 = 6.4^\circ$  and  $a2 = 171.6^\circ$ ) with a P-P distance of  $6.31 \text{ \AA}$ . A second minimum ( $E_{\text{int}} = -186.28 \text{ kcal/mol}$ ) where the ethanol molecule interacted with the acidic  $\text{H}_2$  atom of one of the rings was found. In this case, the rings were rather parallel ( $a1 = 26.0^\circ$ ) and slightly rotated ( $a2 = 159.3^\circ$ ). The relative position of the anions with respect to the rings was the same as in the first minimum. The ethanol molecule was located between the  $\text{PF}_6^-$  anions but only interacting with one of them.

Finally, the  $[\text{CH}_3\text{SO}_3\text{Bmim}]_2 + \text{EtOH}$  aggregates were studied. As in the previous cases, the most stable situation was that with the rings positioned almost in parallel ( $a1 = 174.9^\circ$ ) and with the ethanol molecule interacting with one of the anions and with the  $\text{H}_3$  atom of one of the rings. In this case, the imidazolium rings were turned to each other ( $a2 = 122.2^\circ$ ) and the  $\text{CH}_3\text{SO}_3^-$  species were above and below them with a S-S distance of  $7.79 \text{ \AA}$ . The following minimum is less stable by  $3.68 \text{ kcal/mol}$ . In this case, the planes containing the rings formed an angle  $a1 = 55.3^\circ$  and their orientation was given by the angle  $a2 = 54.9^\circ$ . One  $\text{CH}_3\text{SO}_3^-$  anion was above the imidazolium rings and the other  $\text{CH}_3\text{SO}_3^-$  anion was over one ring. The ethanol molecule only interacted with the  $\text{H}_3$  atom of one ring and with one  $\text{CH}_3\text{SO}_3^-$  anion. The S-S distance was  $6.0 \text{ \AA}$ .

In all  $[\text{XBmim}]_2 + \text{EtOH}$  aggregates, the most stable structure accounts for the interaction of the ethanol molecule with the  $\text{H}_3$  atom of one of the rings rather than with the most acidic hydrogen atom in the ring, the  $\text{H}_2$  atom. This can be motivated by the large size of the cosolvent molecule that restricted to certain extent the cation-anion stabilization when located close to the  $\text{H}_2$  atom. The fact that ethanol molecule only had two sites for strong hydrogen bond interaction and both of them were located at the same side of the molecule can be also an issue to take into account. The most stable  $[\text{XBmim}]_2 + \text{EtOH}$  aggregates had the butyl chains opposite to each other. This made easier the interaction between the ethanol molecule and the  $\text{H}_3$  atom. The comparison of the anion-anion distances in the  $[\text{XBmim}]_2$ ,  $[\text{XBmim}]_2 + \text{H}_2\text{O}$ , and  $[\text{XBmim}]_2 + \text{EtOH}$  aggregates indicated that species containing  $\text{BF}_4^-$  and  $\text{PF}_6^-$  anions barely changed anion distances whereas  $\text{Cl}^-$  and  $\text{CH}_3\text{SO}_3^-$  anions were far away in the case of the  $[\text{XBmim}]_2 + \text{EtOH}$  clusters. Again, the interaction energies were closer in value for  $\text{Cl}^-$  and  $\text{CH}_3\text{SO}_3^-$  species and larger than those for  $\text{BF}_4^-$  and  $\text{PF}_6^-$  aggregates. Similar to the monomers + cosolvent, the interaction energies for  $[\text{XBmim}]_2 + \text{H}_2\text{O}$  or  $\text{EtOH}$  clusters depended on the anion but not on the cosolvent (see Table 1 for details).

## SUMMARY AND CONCLUSIONS

$[\text{BF}_4\text{Bmim}]$  and  $[\text{PF}_6\text{Bmim}]$  ILs were tested as templates in the synthesis of zeolites. Opposite to  $[\text{ClBmim}]$  and  $[\text{CH}_3\text{SO}_3\text{Bmim}]$  ILs, the results showed that these ILs failed

in their role of structure directing agents. Explaining this different behavior in terms of local structure organization of the water/IL and ethanol/ILs mixtures was attempted. To do so, a quantum chemical study of  $[\text{XBmim}]$  (X being  $\text{Cl}$ ,  $\text{BF}_4$ ,  $\text{PF}_6$ , or  $\text{CH}_3\text{SO}_3$ ) ILs interacting with water or ethanol was carried out. To characterize the preferred interaction sites and the relative position of cation-anion-cosolvent,  $[\text{XBmim}]$ ,  $[\text{XBmim}] + \text{H}_2\text{O}$ ,  $[\text{XBmim}] + \text{EtOH}$ ,  $[\text{XBmim}]_2$ ,  $[\text{XBmim}]_2 + \text{H}_2\text{O}$ , and  $[\text{XBmim}]_2 + \text{EtOH}$  aggregates were analyzed. The anion-cosolvent interacted via hydrogen bond in all cases. The cation-cosolvent interaction was more elusive and it was dependent on the interaction of the anion(s) and cosolvent with alkyl chains.

Structural differences among  $[\text{XBmim}]$  aggregates by themselves and plus the cosolvent were found. The position of the anion with respect to the cation was either being over it or in plane with it and depended on the number of species in the cluster and on all the possible interactions, including those of the anion, cation, and cosolvent with the alkyl chains. In a very general way, the  $\text{Cl}^-$  aggregates behaved in a different manner in comparison to the rest of the anions in the sense that structures with  $\text{Cl}^-$  anion closer to the  $\text{H}_2$  atom of the ring were more stable than those with the cosolvent closer to the same atom (although some exceptions can be found) and it preferred to be in the same plane of the imidazolium ring. This did not occur in the case of the  $\text{CH}_3\text{SO}_3^-$  anion that behaved like  $\text{BF}_4^-$  and  $\text{PF}_6^-$  aggregates. Although there was not a specific pattern based on local structures that allowed us to explain the different behavior of these ILs as a zeolite structure template, our results revealed that no matter the size of the aggregate and the nature of the cosolvent the interaction energies involving  $\text{Cl}^-$  and  $\text{CH}_3\text{SO}_3^-$  anions were closer and larger than those for  $\text{BF}_4^-$  and  $\text{PF}_6^-$  species. What's more, they depended on the anion but not on the cosolvent. These differences and similarities in energy can be used as an argument to describe their different behavior as templates. In this sense, the largest  $E_{\text{int}}$  for  $\text{Cl}^-$  and  $\text{CH}_3\text{SO}_3^-$  anions can induce the formation of a stable structure that play the role of structure directing agent whereas the more elusive interaction in the case of  $\text{BF}_4^-$  and  $\text{PF}_6^-$  species was not able to supply the required ingredients to a successful synthesis of zeolites.

When the previous reasoning lines were put together in order to obtain a general view for the controlling factor of the clusters formation, something more than the pure intermolecular interaction appeared to play an important role: the topology of the solvent molecule. In the case of the water molecule, it had three specific sites for interaction with a double-donor capability to form hydrogen bonding and double acceptor capability to accept hydrogen bonding, whereas ethanol only had two sites for strong hydrogen bonding interaction, one of them as donor and the other as double acceptor group. In addition, the size of the ethanol molecule precluded a fair adaptability to coordinate in some positions where the water can fit without disrupting the relative position of the cation vs anion. These features resulted in a certain trend to give rise to opener structures in the case of the ethanol molecules as a cosolvent.

At this point, it is worth pointing out that the inclusion of more cosolvent molecules was not taken into account in this study. This was due to the rapid increase of computational effort, but also to methodological concerns associated to the lack of a proper inclusion of statistical contributions in the quantum mechanical computations. Future studies on this

respect are needed for a better understanding of these systems and they are in progress.

## AUTHOR INFORMATION

### Corresponding Author

\*E-mail: rae@us.es.

### Notes

The authors declare no competing financial interest.

## ACKNOWLEDGMENTS

Financial support for this work has been obtained from Junta de Andalucía (Plan Andaluz de Investigación, grupos TEP106 and FQM282) and the Spanish Ministerio de Ciencia e Innovación ENE 2009-14522-C05-02 cofinanced by FEDER EU funds and CTQ2011-25932. S.I. acknowledges M.E.C. for her contract Ramón y Cajal. CESGA supercomputing center is acknowledged for the computer time, technical expertise, and assistance.

## REFERENCES

- (1) Adams, C. J.; Bradley, A. E.; Seddon, K. R. The Synthesis of Mesoporous Materials Using Novel Ionic Liquid Templates in Water. *Aust. J. Chem.* **2001**, *54*, 679–681.
- (2) Zhou, Y.; Schattka, J. H.; Antonietti, M. Room-Temperature Ionic Liquids as a Template to Monolithic Mesoporous Silica with Wormlike Pores via Sol-Gel Nanocasting Technique. *Nano Lett.* **2004**, *4*, 477–481.
- (3) Zhang, J.; Ma, Y.; Shi, F.; Liu, L.; Deng, Y. Room Temperature Ionic Liquids as Templates in the Synthesis of Mesoporous Silica via a Sol-Gel Method. *Microporous Mesoporous Mater.* **2009**, *119*, 97–103.
- (4) Karout, A.; Pierre, A. C. Silica Xerogels and Aerogels Synthesized with Ionic Liquids. *J. Non-Cryst. Solids* **2007**, *353*, 2900–2909.
- (5) Ma, Z.; Yu, J.; Dai, S. Preparation of Inorganic Materials Using Ionic Liquids. *Adv. Mater.* **2010**, *22*, 261–285.
- (6) Parnham, E. R.; Morris, R. E. Ionothermal Synthesis of Zeolites, Metal-Organic Frameworks, and Inorganic-Organic Hybrids. *Acc. Chem. Res.* **2007**, *40*, 1005–1013.
- (7) Morris, R. E. Ionic Liquids and Microwaves—Making Zeolites for Emerging Applications. *Angew. Chem., Int. Ed.* **2008**, *47*, 442–444.
- (8) Morris, R. E. Ionothermal Synthesis-Ionic Liquids as Functional Solvents in the Preparation of Crystalline Materials. *Chem. Commun.* **2009**, 2990–2998.
- (9) Cooper, E. R.; Andrews, C. D.; Wheatley, P. S.; Webb, P. B.; Wormald, P.; Morris, E. R. Ionic liquids and Eutectic Mixtures as Solvent and Template in the Synthesis of Zeolite Analogue. *Nature* **2004**, *430*, 1012–1016.
- (10) Shayib, R. M.; George, N. C.; Seshadri, R.; Burton, A. W.; Zones, S. I.; Chmelka, B. F. Structure-Directing Roles and Interactions of Fluoride and Organocations with Siliceous Zeolite Frameworks. *J. Am. Chem. Soc.* **2011**, *133*, 18728–18741.
- (11) Martinez Blanes, J. M.; Szyja, B. N.; Romero-Sarria, F.; Centeno, M. A.; Hensen, E. J. M.; Odriozola, J. A.; Ivanova, S. Multiple Zeolite Structures from One Ionic Liquid Template. *Chem.—Eur. J.* **2013**, *19*, 2122–213.
- (12) Cao, Y.; Chen, Y.; Sun, X.; Zhang, Z.; Mu, T. Water Sorption in Ionic Liquids: Kinetics, Mechanisms and Hydrophilicity. *Phys. Chem. Chem. Phys.* **2012**, *14*, 12252–12262.
- (13) Ortega, J.; Vreekamp, R.; Elena, M.; Eduvigis, P. Thermodynamic Properties of 1-Butyl-3-methylpyridinium Tetrafluoroborate and Its Mixtures with Water and Alkanols. *J. Chem. Eng. Data* **2007**, *52*, 2269–2276.
- (14) Fend, S.; Voth, G. A. Molecular Dynamics Simulations of Imidazolium-Based Ionic Liquid/Water Mixtures: Alkyl Side Chain Length and Anion Effects. *Fluid Phase Equilib.* **2010**, *294*, 148–156.
- (15) Bhargava, B. L.; Yasaka, Y.; Klein, M. L. Computational Studies of Room Temperature Ionic Liquid–Mixtures. *Chem. Commun.* **2011**, *47*, 6228–6241.
- (16) Cammarata, L.; Kazarian, S. G.; Salter, P. A.; Welton, T. Molecular States of Water in Room Temperature Ionic Liquids. *Phys. Chem. Chem. Phys.* **2001**, *3*, 5192–5200.
- (17) Hanke, C. G.; Lynden-Bell, R. M. A Simulation Study of Water-Dialkylimidazolium Ionic Liquid Mixtures. *J. Phys. Chem. B* **2003**, *107*, 10873–10878.
- (18) Jiang, W.; Wang, Y.; Voth, G. A. Molecular Dynamics Simulation of Nanostructural Organization in Ionic Liquid/Water Mixtures. *J. Phys. Chem. B* **2007**, *111*, 4812–4818.
- (19) Bernardes, C. E. S.; Minas da Piedade, M. E.; Canongia Lopes, J. N. The Structure of Aqueous Solutions of a Hydrophilic Ionic Liquid: The Full Concentration Range of 1-Ethyl-3-methylimidazolium Ethylsulfate and Water. *J. Phys. Chem. B* **2011**, *115*, 2067–2074.
- (20) Schroeder, C.; Rudas, T.; Neumayr, G.; Benkner, S.; Steinhauser, O. On the Collective Network of Ionic Liquid/Water Mixtures. I. Orientational Structure. *J. Chem. Phys.* **2007**, *127*, 234503–234509.
- (21) Zahn, S.; Wendler, K.; Delle Site, L.; Kirchner, B. Depolarization of Water in Protic Ionic Liquids. *Phys. Chem. Chem. Phys.* **2011**, *13*, 15083–15093.
- (22) Zhong, X.; Fan, Z.; Liu, Z.; Cao, D. Local Structure Evolution and Its Connection to Thermodynamic and Transport Properties of 1-Butyl-3-methylimidazolium Tetrafluoroborate and Water Mixtures by Molecular Dynamics Simulation. *J. Phys. Chem. B* **2012**, *116*, 3249–3263.
- (23) Zhang, Q.; Wang, N.; Wang, S.; Yu, Z. Hydrogen Bonding Behaviors of Binary Systems Containing the Ionic Liquid 1-Butyl-3-methylimidazolium Trifluoroacetate and Water/Methanol. *J. Phys. Chem. B* **2011**, *115*, 11127–11136.
- (24) Zhang, L.; Xu, Z.; Wang, Y.; Li, H. Prediction of the Solvation and Structural Properties of Ionic Liquids in Water by Two-Dimensional Correlation Spectroscopy. *J. Phys. Chem. B* **2008**, *112*, 6411–6419.
- (25) Moreno, M.; Castiglione, F.; Mele, A.; Pasqui, C.; Raos, G. Interaction of Water with the Model Ionic Liquid [bmim][BF<sub>4</sub>]: Molecular Dynamics Simulations and Comparison with NMR Data. *J. Phys. Chem. B* **2008**, *112*, 7826–7836.
- (26) Bowers, J.; Butts, C. P.; Martin, P. J.; Vergara-Gutierrez, M. C.; Heenan, R. K. Aggregation Behavior of Aqueous Solutions of Ionic Liquids. *Langmuir* **2004**, *20*, 2191–2198.
- (27) Kempter, V.; Kirchner, B. The Role of Hydrogen Atoms in Interactions Involving Imidazolium-Based Ionic Liquids. *J. Mol. Struct.* **2010**, *972*, 22–34.
- (28) Fang, D. W.; Sun, Y. C.; Wang, Z. W. Solution Enthalpies of Ionic Liquid 1-Hexyl-3-methylimidazolium Chloride. *J. Chem. Eng. Data* **2008**, *53*, 259–261.
- (29) Mendez-Morales, T.; Carrete, J.; Cabeza, O.; Gallego, L. J.; Varela, L. M. Molecular Dynamics Simulations of the Structural and Thermodynamic Properties of Imidazolium-Based Ionic Liquid Mixtures. *J. Phys. Chem. B* **2011**, *115*, 11170–11182.
- (30) Carrete, J.; Mendez-Morales, T.; Cabeza, O.; Lynden-Bell, R. M.; Gallego, L. G.; Varela, L. M. Investigation of the Local Structure of Mixtures of an Ionic Liquid with Polar Molecular Species through Molecular Dynamics: Cluster Formation and Angular Distributions. *J. Phys. Chem. B* **2012**, *116*, 5941–5950.
- (31) Wu, B.; Zhang, Y.; Wang, H. Insight into the Intermolecular Interactions in [Bmim]BF<sub>4</sub>/[Amim]Cl-Ethanol-Water Mixtures by Near-Infrared Spectroscopy. *J. Phys. Chem. B* **2010**, *113*, 12332–12336.
- (32) Mendez-Morales, T.; Carrete, J.; Garcia, M.; Cabeza, O.; Gallego, L. J.; Varela, L. M. Dynamical Properties of Alcohol + 1-Hexyl-3-methylimidazolium Ionic Liquid Mixtures: A Computer Simulation Study. *J. Phys. Chem. B* **2011**, *115*, 15313–15322.
- (33) Raabea, G.; Köhler, J. Thermodynamical and Structural Properties of Binary Mixtures of Imidazolium Chloride Ionic Liquids and Alcohols from Molecular Simulation. *J. Chem. Phys.* **2008**, *129*, 144503–144508.

- (34) Danten, Y.; Cabaco, M. I.; Besnard, M. Interaction of Water Highly Diluted in 1-Alkyl-3-methyl Imidazolium Ionic Liquids with the  $\text{PF}_6^-$  and  $\text{BF}_4^-$  Anions. *J. Phys. Chem. A* **2009**, *113*, 2873–2889.
- (35) Becke, A. D. Density Functional Thermochemistry. III. The Role of Exact Exchange. *J. Chem. Phys.* **1993**, *98*, 5648–5652.
- (36) Lee, C. T.; Yang, W. T.; Parr, R. G. Development of the Colle-Salvetti Correlation-Energy Formula into a Functional of the Electron Density. *Phys. Rev. B* **1988**, *37*, 785–789.
- (37) Frisch, M. J.; Trucks, G. W.; Schlegel, H. B.; Scuseria, G. E.; Robb, M. A.; Cheesman, J. R.; Zakrzewski, V. G.; Montgomery, J. A., Jr.; Stratmann, R. E.; Burant, J. C.; et al. *Gaussian 03*, Revision E.01; Gaussian Inc.: Pittsburgh, PA, 2003.
- (38) Raju, S. G.; Balasubramanian, S. Aqueous Solution of  $[\text{bmim}][\text{PF}_6]$ : Ion and Solvent Effects on Structure and Dynamics. *J. Phys. Chem. B* **2009**, *113*, 4799–4806.
- (39) Tsuzuki, S.; Tokuda, H.; Hayamizu, K.; Watanabe, M. Magnitude and Directionality of Interaction in Ion Pairs of Ionic Liquids: Relationship with Ionic Conductivity. *J. Phys. Chem. B* **2005**, *109*, 16474–16481.
- (40) Zahn, D.; Kirchner, B. Validation of Dispersion Corrected DFT-Approaches for Ionic Liquid Systems. *J. Phys. Chem. A* **2008**, *112*, 8430–8435.
- (41) Wu, B.; Liu, Y.; Zhang, Y.; Wang, H. Probing Intermolecular Interactions in Ionic Liquid–Water Mixtures by Near-Infrared Spectroscopy. *Chem.—Eur. J.* **2009**, *15*, 6889–6893.
- (42) Heimer, N. E.; Sesto, R. E. D.; Meng, Z.; Wilkes, J. S.; Carper, W. R. Vibrational Spectra of Imidazolium Tetrafluoroborate Ionic Liquids. *J. Mol. Liq.* **2006**, *124*, 84–95.
- (43) Meng, Z.; Dölle, A.; Carper, W. R. Gas Phase Model of an Ionic Liquids: Semi-Empirical and *Ab Initio* Bonding and Molecular Structure. *J. Mol. Struct. (THEOCHEM)* **2002**, *585*, 119–128.
- (44) Morrow, T. I.; Maginn, E. J. Molecular Dynamics Study of the Ionic Liquid 1-n-butyl-3-methylimidazolium Hexafluorophosphate. *J. Phys. Chem. B* **2002**, *106*, 12807–12813.
- (45) Katsyuba, S. A.; Dyson, P. J.; Vandyukova, E. E.; Chernova, A. V.; Vidis, A. Molecular Structure, Vibrational Spectra, and Hydrogen Bonding of the Ionic Liquid 1-Ethyl-3methyl-1H-imidazolium Tetrafluoroborate. *Helv. Chim. Acta* **2004**, *87*, 2556–2565.
- (46) Talaty, R.; Raja, S.; Storhaug, V. J.; Dölle, A.; Carper, W. R. Raman and Infrared Spectra and *Ab Initio* Calculations of  $C_{2-4}\text{MIM}$  Imidazolium Hexafluorophosphate Ionic Liquids. *J. Phys. Chem. B* **2004**, *108*, 13177–13184.
- (47) Berg, R. W.; Deetlefs, M.; Seddon, K. R.; Shim, I.; Thompson, J. M. Raman and *Ab Initio* Studies of Simple and Binary 1-Alkyl-3-methylimidazolium Ionic Liquids. *J. Phys. Chem. B* **2005**, *109*, 19018–19025.
- (48) Umebayashi, Y.; Fujimori, T.; Sukizaki, T.; Asada, M.; Fujii, K.; Kanzaki, R.; Ishiguro, S. Evidence of Conformational Equilibrium of 1-Ethyl-3-methylimidazolium in Its Ionic Liquid Salts: Raman Spectroscopic Study and Quantum Chemical Calculations. *J. Phys. Chem. A* **2005**, *109*, 8976–8982.
- (49) Tsuzuki, S.; Tokuda, H.; Hayamizu, K.; Watanabe, M. Magnitude and Directionality of Interaction in Ion Pairs of Ionic Liquids: Relationship with Ionic Conductivity. *J. Phys. Chem. B* **2005**, *109*, 16474–16481.
- (50) Takamuku, T.; Kyoshin, Y.; Shimomura, T.; Kittaka, S.; Yamaguchi, T. Effect of Water on Structure of Hydrophilic Imidazolium-Based Ionic Liquid. *J. Phys. Chem. B* **2009**, *113*, 10817–10824.
- (51) Spickermann, C.; Thar, J.; Lehmann, S. B. C.; Zahn, S.; Hunger, J.; Buchner, R.; Hunt, P. A.; Welton, T.; Kirchner, B. Why Are Ionic Liquid Ions Mainly Associated in Water? A Car-Parrinello Study of 1-Ethyl-3-methyl-imidazolium Chloride Water Mixture. *J. Chem. Phys.* **2008**, *129*, 104505–104517.